

Constraining Heavy Axionlike Particles by Energy Deposition in Globular Cluster Stars

Giuseppe Lucente^{1,2,*} Oscar Straniero^{3,4,†} Pierluca Carenza^{5,‡} Maurizio Giannotti^{6,§} and Alessandro Mirizzi^{1,2,||}

¹*Dipartimento Interateneo di Fisica “Michelangelo Merlin,” Via Amendola 173, 70126 Bari, Italy*


²*Istituto Nazionale di Fisica Nucleare—Sezione di Bari, Via Orabona 4, 70126 Bari, Italy*

³*INAF, Osservatorio Astronomico d’Abruzzo, 64100 Teramo, Italy*

⁴*Istituto Nazionale di Fisica Nucleare—Sezione di Roma, Piazzale Aldo Moro 2, 00185 Roma, Italy*

⁵*The Oskar Klein Centre, Department of Physics, Stockholm University, AlbaNova, SE-10691 Stockholm, Sweden*

⁶*Department of Chemistry and Physics, Barry University, 11300 NE 2nd Ave., Miami Shores, Florida 33161, USA*

 (Received 12 March 2022; revised 4 May 2022; accepted 13 June 2022; published 29 June 2022)

Heavy axionlike particles (ALPs) with masses up to a few 100 keV and coupled with photons can be efficiently produced in stellar plasmas. We present a new “ballistic” recipe that covers both the energy-loss and energy-transfer regimes, and we perform the first dedicated simulation of Globular Cluster stars including the ALP energy transfer. This argument allows us to constrain ALPs with $m_a \lesssim 0.4$ MeV and $g_{a\gamma} \simeq 10^{-5}$ GeV⁻¹, probing a section of the ALP parameter space informally known as the “cosmological triangle”. This region is particularly interesting since it has been excluded only using standard cosmological arguments that can be evaded in nonstandard scenarios.

DOI: [10.1103/PhysRevLett.129.011101](https://doi.org/10.1103/PhysRevLett.129.011101)

Introduction.—Axions and axionlike particles (ALPs) are ubiquitous in modern particle physics (see, e.g., Refs. [1,2]). The term ALP usually refers to general pseudoscalar particles a , with a two-photon vertex

$$\mathcal{L}_{a\gamma} = -\frac{1}{4}g_{a\gamma}aF_{\mu\nu}\tilde{F}^{\mu\nu}, \quad (1)$$

where a is the ALP field, F is the electromagnetic field strength tensor, \tilde{F} its dual, and $g_{a\gamma}$ is the ALP-photon coupling. Astrophysical arguments offer complementary opportunities to probe the ALP parameter space [3–8] in comparison with other experimental searches [9–20]. In particular, Globular Cluster (GC) stars have been recognized long ago as powerful astrophysical laboratories for ALPs coupled to photons [4,5,21]. Such coupling would allow for an efficient production in the stellar plasma, leading to an additional channel of energy loss and thus altering the stellar evolution. Consequently, the number of stars found in the different evolutionary phases in GCs provides a valuable tool to investigate exotic energy losses in stellar interiors. In this context, the GC R parameter, defined as the number ratio of horizontal branch (HB) to red giant branch (RGB) stars

$$R = \frac{N_{\text{HB}}}{N_{\text{RGB}}}, \quad (2)$$

has been used for a long time to constrain $g_{a\gamma}$.

Light ALPs, with $m_a \lesssim 30$ keV, are produced mainly through the Primakoff process $\gamma + Ze \rightarrow \gamma + a$, i.e., the conversion of a photon into an ALP in the electric field of ions and electrons in the stellar plasma. This process is considerably more efficient in HB than in RGB stars, where it is suppressed by the large plasma frequency and by electron degeneracy. Therefore, for a sufficiently large ALP-photon coupling, the ALP emission would accelerate the stellar evolution in the HB stage, leaving the RGB phase essentially unchanged and thus leading to a reduction of the R parameter. Comparison with the photometric data for 39 GCs leads to the bound $g_{a\gamma} \lesssim 6.6 \times 10^{-11}$ GeV⁻¹ [22,23].

The Primakoff production of heavy ALPs, with $m_a \gtrsim 30$ keV, is Boltzmann suppressed, so that the bound unavoidably relaxes for $m_a \gg T$. However, the reduction of the ALP flux at large masses is partially compensated by the emergence of another ALP production mechanism, the photon coalescence, $\gamma\gamma \rightarrow a$. Though, being thermal, this process suffers from the Boltzmann suppression just like the Primakoff, the steep mass dependence of the coalescence rate [see Eq. (3)] makes it the dominant ALP production mechanism for $m_a \gtrsim 50$ keV. The photon coalescence process was included for the first time in the study of the HB bound on ALPs in Ref. [24]. In that study, free-streaming ALPs were included in the GC simulation as a source of energy loss, and the effect of the ALP decay, $a \rightarrow \gamma\gamma$, was accounted for only as a reduction of the lost energy.

A phenomenological bound was then obtained by searching for the $(m_a, g_{a\gamma})$ pairs for which the ALP mean free path (MFP) was smaller than the convective core

Published by the American Physical Society under the terms of the Creative Commons Attribution 4.0 International license. Further distribution of this work must maintain attribution to the author(s) and the published article’s title, journal citation, and DOI. Funded by SCOAP³.

(A similar strategy was followed in Ref. [25] to constrain ALPs using the white dwarf initial-final mass relation, obtaining bounds comparable to ours.), without evaluating the impact that the energy deposition within the star would have on its evolution. However, for values of large enough couplings and masses a significant fraction of ALPs is expected to decay inside the star. This effect leads to an energy transfer within the star, where ALPs are produced at a given position and deposit their energy by decay into photons at another position. Thus, a reliable description of the ALP impact on the evolution of HB stars cannot, in general, ignore the effects of the ALP-induced energy transport. The energy transport in stellar interior due to exotic particles is usually described as a radiative energy transfer. For different but complementary approaches see Refs. [26–29]. In practice, it is treated as a diffusive phenomenon, by including an exotic component in the evaluation of the radiative opacity (cf. Sec. 1.3.3 in Ref. [4]). However, if the free-streaming approximation is valid when the ALP MFP is comparable or larger than the stellar radius, the diffusive approach requires an ALP MFP smaller than the characteristic temperature (or pressure) scale height. In principle, one can treat separately free-streaming and diffusive ALP regimes, but both these assumptions fail in the case of intermediate ALP MFP. For this reason, instead of considering two different recipes, here we propose a novel *ballistic* model valid for any MFP value. An algorithm based on this model of the ALP energy transport has been included into the full network stellar evolution code (FUNS, see Ref. [30]) and used to calculate new HB stellar models. Though we apply our strategy to the study of the impact of ALPs on the evolution of HB stars, our method is quite general and can be adopted in other cases of exotic energy transport in stars. In general, one expects the ALP energy deposition to become especially relevant for $m_a \sim 0.4$ MeV and $g_{a\gamma} \gtrsim 10^{-6}$ GeV $^{-1}$. These values lay in a region, informally known as the “cosmological triangle” ($m_a \sim 0.5$ – 1 MeV and $g_{a\gamma} \sim 10^{-5}$ GeV $^{-1}$), which, though in tension with standard cosmological arguments [31,32], is hard to access with astrophysical considerations and current experimental searches (see, e.g., Ref. [33]). At small masses, the cosmological triangle is bounded by the HB bound, which we are going to revise in this paper. The situation is shown in Fig. 1. The excluded region from HB stars, derived with our novel method which we will describe below, is shaded in light red and delimited by the continuous red line. The dotted line inside this region shows the previous bound, from the analysis in Ref. [24]. Although, at a first look, it may appear that our new procedure does not change the previous result substantially, the similarity is purely accidental. In fact, the analysis in Ref. [24] is based on the crude assumption that the ALP energy loss becomes negligible when the ALP MFP is smaller than the HB convective core radius, thus neglecting effects of the ALP

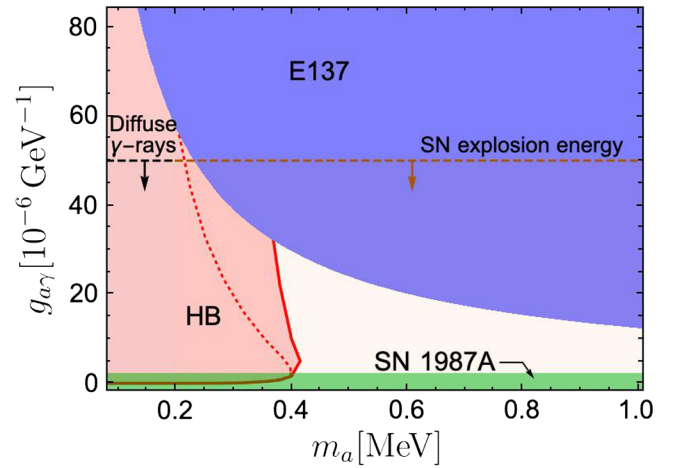


FIG. 1. Overview of the parameter space around the cosmological triangle. See text for more details.

energy deposition and, in turn, of the consequent energy redistribution within the central convective zone. We also notice that the cosmological triangle is bounded at small couplings by the region (in light green) excluded by Supernova (SN) 1987A in the regime of ALPs trapped in the SN core [34], while at larger couplings by the parameters (in blue) excluded by direct searches at beam dump experiments [11,19,20]. By requiring that the energy deposited by decaying ALPs in the outer envelopes of the SN progenitor star must be lower than the SN explosion energy $E_{SN} \sim 10^{51}$ erg, couplings $g_{a\gamma} \lesssim 5 \times 10^{-5}$ GeV $^{-1}$ for $m_a \lesssim 10$ MeV would be excluded [34] (orange dashed band in Fig. 1). However, since a self-consistent SN simulation including ALP energy deposition is not yet available, it is worth using another independent approach to probe this region.

ALP emissivity.—In this Letter, we are mostly concerned with massive ALPs, in the region of the cosmological triangle. As discussed above, the dominant production rate in this regime is the photon coalescence process, $\gamma\gamma \rightarrow a$ (see Ref. [24]), while the Primakoff process can be neglected. In this case, the ALP production rate per unit volume and for ALP energy between E and $E + dE$ is

$$\frac{d\dot{n}_a}{dE} = \frac{g_{a\gamma}^2}{128\pi^3} m_a^4 p \left(1 - \frac{4\omega_{pl}^2}{m_a^2}\right)^{3/2} e^{-E/T}, \quad (3)$$

where ω_{pl} is the plasma frequency, $p = \sqrt{E^2 - m_a^2}$ is the ALP momentum, and the photon distributions are approximated as Maxwell-Boltzmann.

In the following, the plasma frequency will be neglected since in a HB star $\omega_{pl} \lesssim O(10)$ keV, much smaller than the mass $m_a > 100$ keV we are interested in. From Eq. (3), the ALP emissivity (per unit mass) is given by the following expression:

$$\varepsilon_a = \frac{1}{\rho} \int_{m_a}^{\infty} dE E \frac{d\dot{n}_a}{dE}, \quad (4)$$

where ρ is the matter density.

ALP energy deposition.—ALPs produced in the stellar core may decay into photons before leaving the star, depositing energy inside it. This important aspect was never properly addressed in previous investigations. Only in Ref. [24] some attempts were made to account for energy deposition in the stellar core through ALP decay, however with the simplified assumption that only ALPs decaying beyond the convective zone would contribute to the energy loss. To carry our more realistic analysis self-consistently, we now include the effects of the energy deposited by the decaying ALPs directly into the stellar simulations. This allows us to check quantitatively all the outcomes of this energy deposition as well as the stellar feedback on the ALP production. Here we describe the ballistic method we adopt. We assume that ALPs are isotropically emitted, and we model the decay probability as an exponential function with a scale given by the ALP decay length [35,36]

$$\begin{aligned} \lambda &= \frac{64\pi}{g_{a\gamma}^2 m_a^3} \frac{E}{m_a} \sqrt{1 - \left(\frac{E}{m_a}\right)^{-2}} \\ &= 0.57 g_5^{-2} m_{100}^{-3} \frac{E}{m_a} \sqrt{1 - \left(\frac{E}{m_a}\right)^{-2}} R_{\odot}, \end{aligned} \quad (5)$$

where $g_5 = g_{a\gamma}/10^{-5} \text{ GeV}^{-1}$, $m_{100} = m_a/100 \text{ keV}$, and $R_{\odot} = 6.957 \times 10^{10} \text{ cm}$ is the solar radius.

Assuming azimuthal symmetry, for ALPs produced at a radius r , the fraction of survived particles at a radius R after traveling a nonradial path l is given by $e^{-l(r,R,\alpha)/\lambda}$, where the path l depends on the production radius r , the decay radius R , and the zenith angle α , defined as the angle between the particle trajectory and the outward radial direction. For numerical purposes, we discretized the star envelope in N shells, each one delimited by the radii R_i and R_{i+1} ($i = 1, \dots, N$, with $R_1 = 0 \text{ km}$ and $R_{N+1} = R_s$, R_s being the star radius). Since ALPs are emitted isotropically, they can propagate forward ($0 \leq \alpha \leq \pi/2$) or backward ($\pi/2 < \alpha \leq \pi$). Therefore, the energy may be deposited in the i th shell by ALPs produced at larger ($r > R_{i+1}$) or lower radii ($r < R_i$). In addition, due to the finite size of the shell, ALPs may decay in the production shell itself ($R_i < r < R_{i+1}$), before escaping from it. The contribution $\Delta L_{i,d}$ to the rate ΔL_i of energy deposited in the i th shell is given by

$$\Delta L_{i,d}(\alpha) = 2\pi \int_{I_{r,d}} dr r^2 \int_{m_a}^{\infty} dE E \frac{d\dot{n}_a(r)}{dE} \chi_d(l, \lambda), \quad (6)$$

where 2π comes from the integration over the azimuthal angle, $I_{r,d}$ is the integration domain for the radius,

$d\dot{n}_a(r)/dE$ is the production rate given by Eq. (3), and $\chi_d(l, \lambda)$ accounts for the fraction of ALPs decaying in the i th shell, depending on the path l and the decay length λ . The explicit forms of $I_{r,d}$ and $\chi_d(l, \lambda)$ depend on the considered contribution. For instance, for *forward emission* ($d = F$) the integration domain is $I_{r,F} = [0, R_{i+1}]$ and

$$\chi_F = \begin{cases} e^{-l(r,R_i,\alpha)/\lambda} - e^{-l(r,R_{i+1},\alpha)/\lambda}, & r \in [0, R_i), \\ 1 - e^{-l(r,R_{i+1},\alpha)/\lambda} & r \in [R_i, R_{i+1}), \end{cases} \quad (7)$$

with the path length l given by

$$l(r, R, \alpha) = -r \cos \alpha + R \sqrt{1 - \left(\frac{r}{R}\right)^2 \sin^2 \alpha}. \quad (8)$$

In Sec. IA of the Supplemental Material [37], we provide details on the contributions related to the *backward emission*. We can compute the total rate of energy deposited in the i th shell as

$$\Delta L_i(\alpha) = \sum_d \Delta L_{i,d}(\alpha), \quad (9)$$

where the sum is over all the possible contributions.

The rate of energy deposited per unit mass in the i th shell is defined as

$$\varepsilon_{\text{dep},i}(\alpha) = \frac{\Delta L_i(\alpha)}{\Delta M_i}, \quad (10)$$

where ΔM_i is the mass enclosed in the i th shell. Finally, the rate of energy deposited per unit mass averaged over the cosine of the emission angle is given by

$$\langle \varepsilon_{\text{dep},i} \rangle = \int_0^{\pi/2} d\alpha \sin \alpha \varepsilon_{\text{dep},i}, \quad (11)$$

where $\alpha \leq \pi/2$, with the backward emission corresponding to $\pi - \alpha$. We evaluate the integral in Eq. (11) with a Gaussian-Legendre N_{α} -point quadrature formula. Our results are obtained fixing $N_{\alpha} = 10$. In Sec. IB of the Supplemental Material [37] we show that this choice is sufficient to guarantee good accuracy in our numerical analysis.

ALP energy transfer in GC stars.—The usual assumption in stellar model computations is that ALPs, once produced in the hot core, escape the star, thus acting as a local energy-loss process. This assumption becomes particularly inadequate if the ALP MFP is smaller than the convective core radius. In this case, the ALP production and decay processes cause an energy redistribution within the core, which reduces the temperature gradient and, in turn, limits the convective instability. In practice, in the case of HB stars the ALP decay cannot be neglected for ALP masses above $m_a \sim 0.4 \text{ MeV}$ and coupling constants above

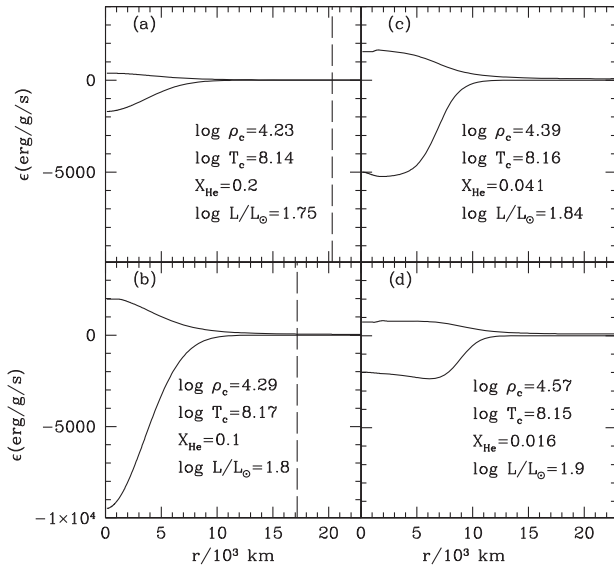


FIG. 2. In each panel, the two curves show, respectively, (i) the energy-loss rate, due to the coalescence process (always negative), and (ii) the energy deposition rate, due to the ALP-decay process (always positive), within the core of a late HB model. The dashed vertical line in panel (a) and (b) marks the location of the external border of the convective core.

$g_{a\gamma} \sim 10^{-6} \text{ GeV}^{-1}$. In Fig. 2, we show the evolution of the rate of energy loss (due to the coalescence process) and the rate of energy deposition (due to the ALP decay) within the convective core of a HB model computed assuming $m_a = 0.4 \text{ MeV}$ and $g_{a\gamma} = 3 \times 10^{-6} \text{ GeV}^{-1}$. In each of the four panels, the corresponding central density and temperature, central He mass fraction, and stellar luminosity are reported. For a large portion of the HB lifetime, the redistribution of the nuclear energy released near the center is dominated by the convective mixing. However, when the central He mass fraction is reduced down to $X_{\text{He}} \sim 0.2$, ALP production and decay start to contribute to the energy transport [Fig. 2(a)]. As a consequence, the temperature gradient becomes smaller and, in turn, the convective instability recedes. The maximum effects is attained when $X_{\text{He}} \sim 0.1$ [Fig. 2(b)]. This causes a premature disappearance of the convective core, although the He burning is still effective near the center, inducing a rapid contraction of the stellar core, not coupled to an increase in the temperature, because of the combined action of ALP and plasma-neutrino production. As a result, the core temperature decreases slightly (the maximum T moves off center), while a substantial increase in the density occurs [Figs. 2(c) and 2(d)].

In Fig. 3, we compare the luminosity evolution of HB models computed assuming different values for m_a and $g_{a\gamma}$. In Ref. [22] it was shown that, assuming a conservative upper limit for the He content of the early galactic gas, $Y = 0.26$, the R parameter obtained from photometric observations of 39 GCs, $R = 1.39 \pm 0.03$, implies the

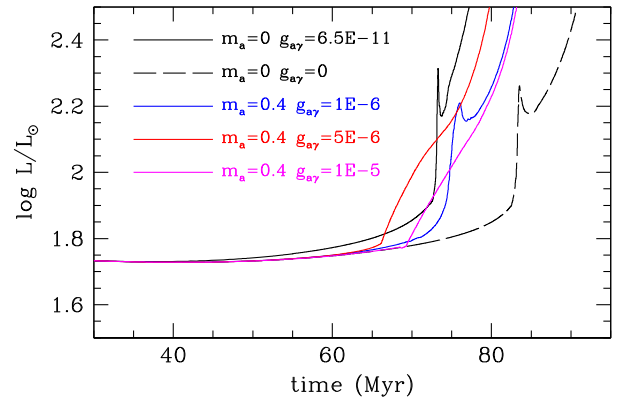


FIG. 3. Luminosity versus time for HB models computed under different assumptions for ALP mass (in MeV) and coupling (in GeV^{-1}), as reported in the inside caption. Time 0 corresponds to the beginning of the He burning.

upper bound $g_{a\gamma} = 0.65 \times 10^{-10} \text{ GeV}^{-1}$ (95% C. L.) for light ALPs ($m_a \lesssim 10 \text{ keV}$). As further discussed in Ref. [24], in order to constrain heavier ALPs, we have evaluated the HB lifetime for a GC benchmark without exotic energy loss (the black-dashed line in Fig. 3) and for a model including light ALPs with $g_{a\gamma} = 0.65 \times 10^{-10} \text{ GeV}^{-1}$ (black-solid line in Fig. 3). Since the value of the R parameter is directly related to the HB lifetime, we can find the ALP bound at any mass in perfect analogy to what was done in the case of light ALPs. Specifically, to find the 95% C.L. we should require that the HB lifetime at any fixed ALP mass is not shorter than the lifetime corresponding to a light ALP with $g_{a\gamma} = 0.65 \times 10^{-10} \text{ GeV}^{-1}$. The comparison with the lifetime of the reference model is done when the stellar luminosity attains $\log L/L_{\odot} = 1.9$, L_{\odot} being the Sun luminosity, a level representative of the upper HB boundary. According to this rule, we find that the bound in Ref. [22] for light ALPs can be reproduced by assuming for instance $m_a = 0.4 \text{ MeV}$ and $g_{a\gamma} = 1.6 \times 10^{-6} \text{ GeV}^{-1}$. Smaller couplings cannot be excluded, because they lead to longer HB lifetimes. This is the case of the $m_a = 0.4 \text{ MeV}$ and $g_{a\gamma} = 10^{-6} \text{ GeV}^{-1}$ model represented by the blue line in Fig. 3. On the contrary, the HB is too short at a larger coupling, as in the case of the model with $m_a = 0.4 \text{ MeV}$ and $g_{a\gamma} = 5 \times 10^{-6} \text{ GeV}^{-1}$ represented by the red line in Fig. 3. However, for even larger couplings (an example is the model shown in magenta in Fig. 3, with $g_{a\gamma} = 1 \times 10^{-5} \text{ GeV}^{-1}$) the HB lifetime begins to increase again. This occurrence is due to the extreme reduction of the ALP MFP that scales as $g_{a\gamma}^{-2}$. Therefore, for high couplings, the ALP MFP becomes so short that most of the ALPs decay very close to their production site, and their contribution to the energy redistribution becomes negligible. Thus, for each value of the ALP mass we get a pair of $g_{a\gamma}$ that reproduce the light ALP bound.

In Sec. II of the Supplemental Material [37] we compare the results obtained with the ballistic method used here with the ones found using the diffusive energy-transfer approach.

Conclusions.—In this Letter, we presented a detailed study of the ALP-induced energy transfer in HB stars including, for the first time, a reliable quantitative analysis of the effects of ALPs decaying into photons inside the stellar core. For this purpose, we developed a simple recipe to model this nonlocal energy transfer process and included it in our numerical simulations. Our study strengthens the ALP-photon bound for masses $m_a \sim 0.4$ MeV, thus restricting the “cosmological triangle.” Though applied to the specific case of HB stars in GCs, our method can be readily extended to other stars, providing a general recipe to describe energy transfer in situations in which neither the free streaming nor the diffuse approximations are fully justified.

We warmly thank G. Raffelt for useful comments on the manuscript. The work of M. G. was partially supported by funding from a grant provided by the Fulbright U.S. Scholar Program. For this work, O. S. has been funded by the Italian Space Agency (ASI) and the Italian National Institute of Astrophysics (INAF) under Agreement No. 2017-14-H.0 -attività di studio per la comunità scientifica di Astrofisica delle AlteEnergie e Fisica Astroparticellare. The work of G. L. and A. M. is partially supported by the Italian Istituto Nazionale di Fisica Nucleare (INFN) through the “Theoretical Astroparticle Physics” project and by research Grant No. 2017W4HA7S “NAT-NET: Neutrino and Astroparticle Theory Network” under the program PRIN 2017 funded by the Italian Ministero dell’Università e della Ricerca (MIUR). The work of P. C. is supported by the European Research Council under Grant No. 742104 and by the Swedish Research Council (VR) under Grants No. 2018-03641 and No. 2019-02337.

* giuseppe.lucente@ba.infn.it

† oscar.straniero@inaf.it

* pierluca.carenza@fysik.su.se

§ MGiannotti@barry.edu

|| alessandro.mirizzi@ba.infn.it

- [1] A. Ringwald, Axions and axion-like particles, in 49th Rencontres de Moriond on Electroweak Interactions and Unified Theories, 2014, [arXiv:1407.0546](https://arxiv.org/abs/1407.0546).
- [2] L. Di Luzio, M. Giannotti, E. Nardi, and L. Visinelli, The landscape of QCD axion models, *Phys. Rep.* **870**, 1 (2020).
- [3] G. G. Raffelt, Astrophysical methods to constrain axions and other novel particle phenomena, *Phys. Rep.* **198**, 1 (1990).
- [4] G. G. Raffelt, *Stars as Laboratories for Fundamental Physics* (Chicago University Press, Chicago, 1996).
- [5] G. G. Raffelt, Astrophysical axion bounds, *Lect. Notes Phys.* **741**, 51 (2008).
- [6] M. Giannotti, I. Irastorza, J. Redondo, and A. Ringwald, Cool WISPs for stellar cooling excesses, *J. Cosmol. Astropart. Phys.* **05** (2016) 057.
- [7] M. Giannotti, I. G. Irastorza, J. Redondo, A. Ringwald, and K. Saikawa, Stellar recipes for axion hunters, *J. Cosmol. Astropart. Phys.* **10** (2017) 010.
- [8] L. Di Luzio, M. Fedele, M. Giannotti, F. Mescia, and E. Nardi, Stellar evolution confronts axion models, *J. Cosmol. Astropart. Phys.* **02** (2022) 035.
- [9] I. G. Irastorza and J. Redondo, New experimental approaches in the search for axion-like particles, *Prog. Part. Nucl. Phys.* **102**, 89 (2018).
- [10] P. Sikivie, Invisible axion search methods, *Rev. Mod. Phys.* **93**, 015004 (2021).
- [11] P. Agrawal *et al.*, Feebly-interacting particles: FIPs 2020 workshop report, *Eur. Phys. J. C* **81**, 1015 (2021).
- [12] V. Anastassopoulos *et al.* (CAST Collaboration), New CAST limit on the axion-photon interaction, *Nat. Phys.* **13**, 584 (2017).
- [13] E. Armengaud *et al.* (IAXO Collaboration), Physics potential of the international axion observatory (IAXO), *J. Cosmol. Astropart. Phys.* **06** (2019) 047.
- [14] A. Abeln *et al.* (BabyIAXO Collaboration), Conceptual design of BabyIAXO, the intermediate stage towards the international axion observatory, *J. High Energy Phys.* **05** (2021) 137.
- [15] T. Braine *et al.* (ADMX Collaboration), Extended Search for the Invisible Axion with the Axion Dark Matter Experiment, *Phys. Rev. Lett.* **124**, 101303 (2020).
- [16] P. Brun *et al.* (MADMAX Collaboration), A new experimental approach to probe QCD axion dark matter in the mass range above $40 \mu\text{eV}$, *Eur. Phys. J. C* **79**, 186 (2019).
- [17] R. Bähre *et al.*, Any light particle search II—Technical Design Report, *J. Instrum.* **8**, T09001 (2013).
- [18] R. Ballou *et al.* (OSQAR Collaboration), New exclusion limits on scalar and pseudoscalar axionlike particles from light shining through a wall, *Phys. Rev. D* **92**, 092002 (2015).
- [19] M. J. Dolan, T. Ferber, C. Hearty, F. Kahlhoefer, and K. Schmidt-Hoberg, Revised constraints and Belle II sensitivity for visible and invisible axion-like particles, *J. High Energy Phys.* **12** (2017) 094; Erratum, *J. High Energy Phys.* **03** (2021) 190.
- [20] B. Döbrich, J. Jaeckel, and T. Spadaro, Light in the beam dump—ALP production from decay photons in proton beam-dumps, *J. High Energy Phys.* **05** (2019) 213; Erratum, **10** (2020) 046.
- [21] G. G. Raffelt and D. S. P. Dearborn, Bounds on hadronic axions from stellar evolution, *Phys. Rev. D* **36**, 2211 (1987).
- [22] A. Ayala, I. Domínguez, M. Giannotti, A. Mirizzi, and O. Straniero, Revisiting the Bound on Axion-Photon Coupling from Globular Clusters, *Phys. Rev. Lett.* **113**, 191302 (2014).
- [23] O. Straniero, A. Ayala, M. Giannotti, A. Mirizzi, and I. Domínguez, Axion-photon coupling: Astrophysical constraints, in *Proceedings of the 11th Patras Workshop on Axions, WIMPs and WISPs* (2015), pp. 77–81, [10.3204/DESY-PROC-2015-02/straniero_oscar](https://arxiv.org/abs/10.3204/DESY-PROC-2015-02/straniero_oscar).
- [24] P. Carenza, O. Straniero, B. Döbrich, M. Giannotti, G. Lucente, and A. Mirizzi, Constraints on the coupling with photons of heavy axion-like-particles from globular clusters, *Phys. Lett. B* **809**, 135709 (2020).

- [25] M. J. Dolan, F. J. Hiskens, and R. R. Volkas, Constraining axion-like particles using the white dwarf initial-final mass relation, *J. Cosmol. Astropart. Phys.* **09** (2021) 010.
- [26] G. G. Raffelt and G. D. Starkman, Stellar energy transfer by keV mass scalars, *Phys. Rev. D* **40**, 942 (1989).
- [27] A. Gould and G. Raffelt, Cosmion energy transfer in stars: The knudsen limit, *Astrophys. J.* **352**, 669 (1990).
- [28] A. Gould and G. Raffelt, Thermal conduction by massive particles, *Astrophys. J.* **352**, 654 (1990).
- [29] A. V. Sokolov, Generic energy transport solutions to the solar abundance problem—a hint of new physics, *J. Cosmol. Astropart. Phys.* **03** (2020) 013.
- [30] O. Straniero, C. Pallanca, E. Dalessandro, I. Dominguez, F. R. Ferraro, M. Giannotti, A. Mirizzi, and L. Piersanti, The RGB tip of galactic globular clusters and the revision of the bound of the axion-electron coupling, *Astron. Astrophys.* **644**, A166 (2020).
- [31] D. Cadamuro and J. Redondo, Cosmological bounds on pseudo Nambu-Goldstone bosons, *J. Cosmol. Astropart. Phys.* **02** (2012) 032.
- [32] P. F. Depta, M. Hufnagel, and K. Schmidt-Hoberg, Robust cosmological constraints on axion-like particles, *J. Cosmol. Astropart. Phys.* **05** (2020) 009.
- [33] V. Brdar, B. Dutta, W. Jang, D. Kim, I. M. Shoemaker, Z. Tabrizi, A. Thompson, and J. Yu, Axionlike Particles at Future Neutrino Experiments: Closing the Cosmological Triangle, *Phys. Rev. Lett.* **126**, 201801 (2021).
- [34] A. Caputo, G. Raffelt, and E. Vitagliano, Muonic boson limits: Supernova redux, *Phys. Rev. D* **105**, 035022 (2022).
- [35] J. Jaeckel, P. C. Malta, and J. Redondo, Decay photons from the axionlike particles burst of type II supernovae, *Phys. Rev. D* **98**, 055032 (2018).
- [36] G. G. Raffelt, Axions: Motivation, limits and searches, *J. Phys. A* **40**, 6607 (2007).
- [37] See Supplemental Material at <http://link.aps.org/supplemental/10.1103/PhysRevLett.129.011101> for a detailed description of the ballistic model (Sec. I) and a comparison between the ballistic model and the diffusive energy-transfer approach (Sec. II).